available at www.sciencedirect.com

ScienceDirect

journal homepage: www.elsevier.com/locate/biochempharm

Interactions of human serum albumin with retinoic acid, retinal and retinyl acetate

Elena Karnaukhova *,[1]

Laboratory of Biochemistry and Vascular Biology, Division of Hematology, Center for Biologics Evaluation and Research, Food and Drug Administration, Bethesda, MD 20892, USA

ARTICLE INFO

Article history:
Received 9 September 2006
Accepted 27 November 2006

Keywords:
Human serum albumin
Retinoic acid
Retinal
Retinyl acetate
Circular dichroism
Protein-induced chirality

ABSTRACT

Human serum albumin (HSA), a major plasma protein and plasma-derived therapeutic, interacts with a wide variety of drugs and native plasma metabolites. In this study the interactions between HSA and small lipophilic molecules *all-trans* retinoic acid (RA), *all-trans* retinaldehyde (retinal, RAL) and *all-trans* retinyl acetate (RAC) were investigated by UV–vis absorption spectroscopy, fluorescence spectroscopy and circular dichroism (CD). This paper focuses on investigation of the interactions between HSA and RA by the visible CD. RAL and RAC were used in this study due to their structural identity to RA to elucidate the importance of the end functional group for the complex formation. Our data demonstrate that RA specifically binds to HSA in a stable non-covalent complex at least at two internal binding sites with close but distinct affinities. Upon titration of HSA with RA, visible CD spectra clearly demonstrate the appearance of a well-defined induced positive Cotton Effect (CE) around 350 nm. Beyond ligand-to-protein ratio of 0.8 and up to saturation (2.0), CD exhibits two major bands of opposite signs, suggesting exciton coupling between the chromophore molecules in the protein interior. The fluorescence quenching data suggest proximity of the primary RA binding site to tryptophan (W^{214}). RAC shows a weak association with HSA with stoichiometry close to that of RA, while interactions of RAL with HSA proceed non-specifically at multiple sites. Contrary to RA, the adducts of HSA with RAC and RAL do not show any induced chirality, thus indicating that despite their high structural similarity to RA, both compounds do not appear to occupy the internal binding sites, but associate with the protein exterior.

Published by Elsevier Inc.

1. Introduction

HSA is one of the best studied plasma proteins that functions primarily to maintain colloid osmotic pressure [1–3]. Due to multiple binding sites, HSA serves as a major plasma carrier for wide variety of endogeneous and exogeneous compounds [3,4]. A great deal of research effort focuses on investigation of the interactions of HSA with various compounds and the nature and the characterization of these binding sites [5–7].

Abundance of HSA in the circulatory system and its extraordinary acceptor capabilities make it an important tool in the prognosis of pharmacokinetic behavior of many drugs.

* Tel.: +1 301 402 4635; fax: +1 301 402 2780.
E-mail address: elena.karnaukhova@fda.hhs.gov.

[1] The opinions and assertions herein are the scientific views of the author and are not to be construed as policy of the United States Food and Drug Administration.

Abbreviations: CD, circular dichroism; CE, Cotton Effect; HSA, human serum albumin; FA, fatty acid; L/P, ligand-to-protein (molar) ratio; PBS, phosphate buffer saline; RA, *all-trans* retinoic acid; RAC, *all-trans* retinyl acetate; RAL, *all-trans* retinaldehyde; UV–vis, absorbance

0006-2952/$ – see front matter. Published by Elsevier Inc.
doi:10.1016/j.bcp.2006.11.023

Often, more than 90% of the drugs are bound to the protein, which significantly influences the drug efficacy, the rate of drug delivery and elimination [2,4,8].

Retinoids, or vitamin A derivatives, are small lipophylic molecules comprised of β-ionone cycle and conjugated polyene chain of four double bonds (Fig. 1). Natural and synthetic retinoids possess a wide spectrum of physiological functions. Besides vision transduction, retinoids play a pivotal role in many biological processes including apoptosis and cell differentiation, control of proliferation, reproduction and morphogenesis [9]. Recent work revealed a key role of RA as a signaling molecule in adult brain [10,11].

In vivo, multiple physiological functions of retinoids are facilitated by specialized retinoid receptors and retinoid-binding proteins [12,13]. Retinoids are known for their extremely low aqueous solubility, instability towards oxygen, light and temperature, and for their toxic effects [14–17]. Due to their broad spectrum of physiological activities, natural and synthetic retinoids are widely used, as well as utilized for developing new treatment strategies for various diseases [18–20].

RA, tretinoin (MW 300.4), is a US FDA-approved orphan drug (Vesanoid®) recommended for the treatment of acute promyelocytic leukemia [21,22]. RA has been tested experimentally for its utility as a chemopreventive and an antineoplastic agent for the treatment of solid tumors, and for various dermatologic uses (e.g., [23,24]). RAL, known as retinal (MW 284.4) and RAC (MW 328.5) are metabolically related to RA [25]. RAC is the commercial form of vitamin A used as a vitamin supplement, and RAL is being developed as a topical preparation [26]. However, according to the available literature, the binding properties of these retinoids towards plasma proteins are not fully investigated. Even though these vitamin A derivatives are available as commercial therapeutics, the protein binding properties and the pharmacokinetic data are likely proprietary industry information.

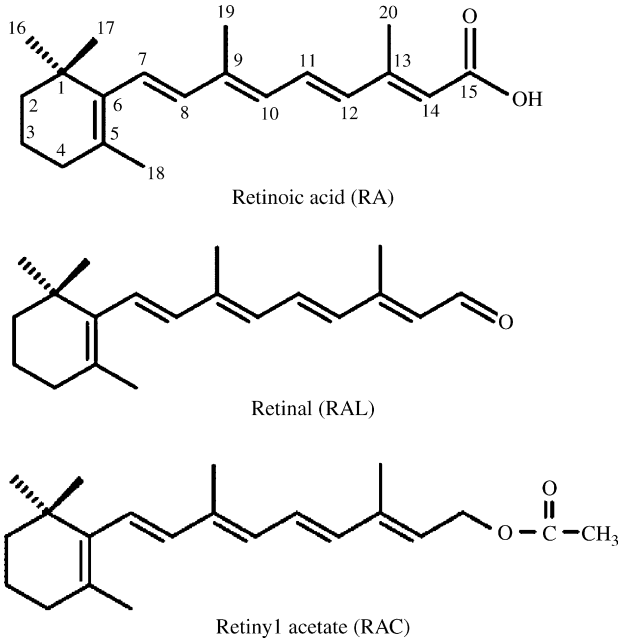

Fig. 1 – *All-trans* retinoids used in the present study.

In order to gain a better understanding of the interactions between HSA with vitamin A derivatives, a complexation of HSA with RA, RAC, and RAL was investigated in this work with the main emphasis on evaluation of these interactions by the visible CD. RAC and RAL were chosen due to their structural identity with RA except for the end functional group, in order to evaluate the impact of substitution of carboxylic group of RA for more reactive carbonyl group or neutral ester on complexation with HSA. This paper presents our results as studied by electronic absorption spectroscopy, fluorescence spectroscopy and CD.

Vitamin A derivatives are excellent optical probes sensitive to conformational distortion that can be detected in 300–600 nm range of CD (often referred as visible CD). The main focus of this study was to examine interactions of chromophoric ligands with protein binding sites by visible CD. While a conventional protein CD in the far-UV range does not reveal any significant changes upon complexation of HSA with RA [27], here we demonstrate that the visible CD reflects dramatic conformational changes of the ligand (chromophore) due to protein-induced chirality and suggests exciton coupling between the RA molecules within the protein.

2. Material and methods

2.1. Materials

Human serum albumin essentially fatty acid free, *all-trans* retinoic acid, *all-trans* retinal and *all-trans* retinyl acetate were purchased from Sigma Chemical Co. (St. Louis, MO, USA). Ethyl alcohol, anhydrous, USP grade was obtained from the Warner-Graham (Cockeysville, MD, USA). Phosphate buffered saline (PBS) pH 7.4 was from Quality Biological Inc. (Gaithersburg, MD, USA). Other chemicals were analytical grade from Fisher Scientific (Fair Lawn, NJ, USA). Greiner 96-well black flat bottom plates (T-3021-12) for fluorescence measurements were from ISC BioExpress (Kaysville, UT, USA).

2.2. Preparation of HSA solutions

The lyophilized protein was reconstituted in water to a concentration of 200 μM, and further dilution to a concentration of 45 μM was performed by adding PBS. This stock solution was aliquoted and stored frozen at −70 °C until use. Concentration of albumin was determined spectrophotometrically using extinction coefficient ($A_{280}^{0.1\%}$ 0.531) [2].

2.3. Preparation of ligand solutions

1.1 mM and 3.3 mM stock solutions of RA, RAL and RAC were prepared in absolute ethanol, degassed under vacuum, purged with argon and stored protected from light at −20 °C. The concentrations of the retinoids in stock solutions were determined spectrophotometrically in ethanol using their extinction coefficients at λ_{max}: 49,700 $M^{-1}\,cm^{-1}$ for RA, 42,400 $M^{-1}\,cm^{-1}$ for RAL [14], and 51,180 $M^{-1}\,cm^{-1}$ for RAC [28].

2.4. Titration of HSA with ligands

For titration of HSA with RA, RAL, and RAC the following protocol was used. For all samples a 45 μM stock solution of HSA in PBS, pH 7.4 was used to provide an equal concentration of 43.2 μM upon adding the ligand(s) in ethanolic solution (or ethanol only for the control protein samples). Adding aliquots of RA (or RAL/RAC) solutions was performed using 1.1 mM and 3.3 mM stock solutions in ethanol to create the set(s) with samples that differ by ~0.1 equiv. of putative ligand, with ligand-to-protein (molar) ratio (L/P) increasing from 0 to 2.0. The volumes, the protein concentration (43.2 μM) and the content of ethanol (<4%, v/v) for all samples were kept the same, thus only the ligand concentration was varied. The titration samples were prepared in 2 mL plastic tubes and incubated in dark, at 25 °C with slow rotation for not less than 4 h. HSA sample containing the same aliquot (78 μL) of ethanol was used as a control; the corresponding spectra were subtracted from the CD and UV–vis spectra of the titration samples. 78 μL of RA (RAL and RAC) stock solutions in ethanol added to 1880 μL of PBS buffer were used as control chromophore samples to monitor spectral changes of each of these retinoids without protein in order to exclude a false interpretation and to confirm that the observed spectral behavior of these compounds differs from that in the presence of HSA.

All titration samples have been monitored by UV–vis and assayed for the induced optical activity and fluorescence quenching.

2.5. UV–vis measurements

UV–vis spectroscopy was performed on Agilent HP8453 UV-visible spectrophotometer (Agilent Technologies Deutschland GmbH, Germany) at 25 °C in the range 200–700 nm using a quartz cuvette with 1 cm pathlength.

2.6. Fluorescence measurements

The fluorescence measurements were carried out using SPECTRAmax GEMINI XS Microplate Spectrofluorometer (Molecular Devices, CA, USA) at 25 °C. Each titration set has been loaded onto the Greiner 96-well black flat bottom plate using 200 μL of each sample *in triplicate*. The excitation wavelength was 295 nm, and the emission spectra were recorded between 300 nm and 500 nm with maximum observed at 340 nm. The bandwidth for measuring emission was 1 nm. Fluorescence of free RA (saturated solution) in PBS, pH 7.4, was equal to the blank (buffer solution). The data analysis was performed using 4.7.1 SOFTmax PRO software.

2.7. CD measurements

CD spectra were recorded between 300 nm and 600 nm on a Jasco J-810 Spectropolarimeter (JASCO Co., Japan) at 25 ± 0.2 °C in a rectangular quartz cuvette with 1 cm pathlength. All spectra were accumulated *in triplicate* with a bandwidth of 1.0 nm and a resolution of 0.2 nm at a scan speed of 100 nm/min. Induced CD was determined as the CD of the HSA–RA complex sample after subtraction of CD of the protein alone.

For measuring CD spectra in the far-UV region, the samples were diluted 10-fold with PBS, and the spectra were recorded between 200 nm and 260 nm in the fore-mentioned conditions using quartz cuvette with 2 mm pathlength. An ellipticity of CD spectra is expressed in millidegrees.

3. Results

3.1. UV–vis absorption spectroscopy

Solubility of retinoid and complex formation. Fig. 2 shows absorption spectra of RA, RAL, and RAC in ethanol. Each of these spectra features a single intense absorption band of relatively broad and vibrationally unresolved shape typical for these retinoids [29,30]. Grey traces reflect solubility of RA, RAL and RAC, respectively in PBS, as measured for their saturated solutions in buffer. Therefore, due to extremely low aqueous solubility of retinoids they were added to the protein preparation in PBS as small aliquots of the concentrated ethanolic stock solutions.

3.1.1. RA

Adding of the RA aliquots to PBS above RA aqueous solubility results in immediate bathochromic shift to 420–440 nm in the absorption spectra (most likely reflecting a micelle formation), followed by a timely shift to 330 nm, with a significant drop of the absorption intensity [12,14]. Upon adding to buffer, RA aggregates and precipitates rapidly (the amount of precipitated RA was estimated from the UV–vis spectra of the ethanolic washes of the vials and/or quartz cuvette).

In contrast, when added to the PBS containing HSA (43.2 μM), RA demonstrates apparent solubility up to 87 μM that is far beyond its aqueous solubility. Titration of HSA with increasing amounts of the RA (from 0.4 μM to 87 μM) results in a proportional increase in the absorption intensities of almost symmetrical electronic spectra at 346 nm (Fig. 3a), the first manifestation of the ligand complexation with protein. An excellent signal-to-noise ratio, the absence of RA precipitation on the vial/cuvette walls and apparent visual clarity of the

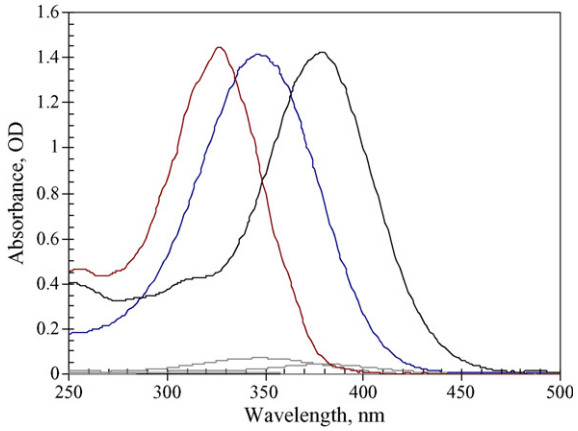

Fig. 2 – UV–vis spectra of RA (λ_{max} 346 nm), RAL (λ_{max} 380 nm), and RAC (λ_{max} 327 nm) in ethanol. Grey traces at the bottom reflect solubility of RA, RAL and RAC in PBS, pH 7.4, respectively.

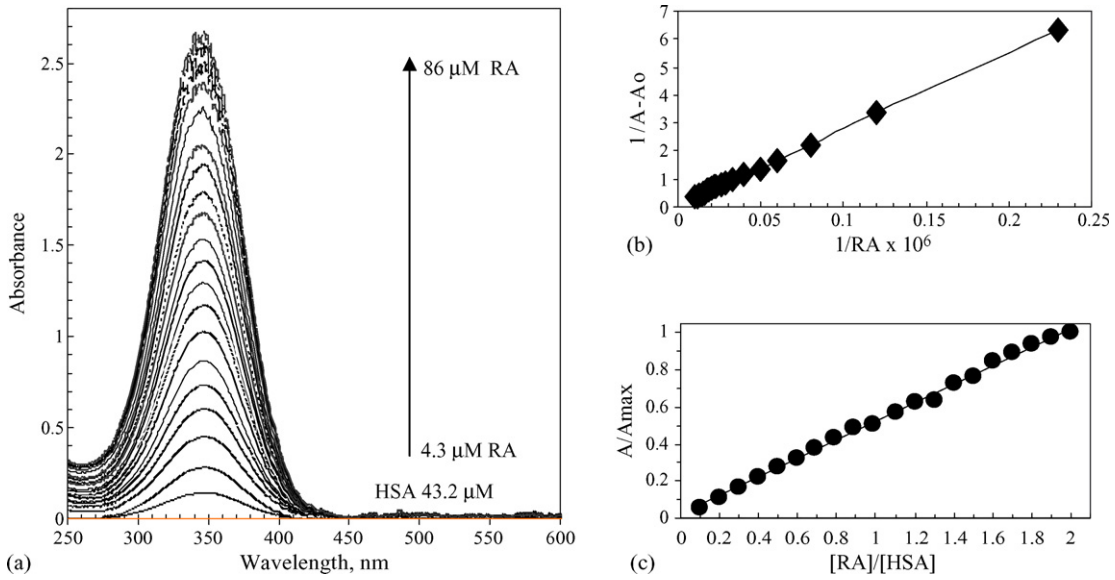

Fig. 3 – UV–vis data of titration of HSA with RA: UV–vis spectra of the has samples containing increasing amounts of RA (spectrum of 43.2 μM HSA is subtracted) (a); double reciprocal plot of the absorption change vs. RA concentration (b); A/A_{max} as a function of L/P (c). The spectra were recorded 8 h later after adding RA.

samples up to the ratio 2 mol of RA per 1 mol of HSA (L/P 2.0), clearly define a stoichiometry of binding (2:1). The increasing RA content in the titration experiments above L/P of 2.0 results in opalescent samples with corresponding changes in UV–vis spectra, which indicates that saturation was achieved.

The absorption intensities at λ_{max} for the HSA–RA samples have been performed as a double reciprocal plot (Fig. 3b) and as a function of RA per HSA (mol/mol) (Fig. 3c), both plots show excellent linearities with r^2 of 1.0 and 0.99, respectively.

The complexes of HSA with RA are highly stable, as demonstrated by the same (100%) intensity and shape of UV–vis spectra after 3 months storage in original solution at 4 °C.

3.1.2. RAC

UV–vis spectra of titration of HSA with RAC reveal an association of RAC (λ_{max} 327 nm) with HSA as observed by a strong absorption at λ_{max} 335 nm upon adding of retinyl acetate (see Section 3.4). The apparent solubility of RAC (up to 85 μM) in the protein solution indicates a stoichiometry close to that of RA (~2 mol per 1 mol of HSA), but UV–vis monitoring shows rapid decrease of the intensity of chromophore band. To exclude the possibility of a false interpretation of UV–vis spectra due to a better solubility of RAC in ethanol–PBS (4% v/v), the samples of RAC in PBS with and without HSA have been monitored in parallel within 20 h under the same conditions. The results revealed that the spectral behavior of RAC associated with HSA and spectral changes of the control RAC sample in PBS proceed quite differently.

3.1.3. RAL

Titration of HSA with RAL has been performed in the same conditions and concentration range as for RA and RAC. Upon reaction with HSA, the absorption maximum of RAL (380 nm) shifts to 375 nm. This hypsochromic shift ~5–6 nm was reproducibly shown for the complexes of L/P 1.0 and 2.0. Complex formation was monitored for all samples of L/P from 0.1 to 2.0 (data not shown), and saturation was not observed. Titration of HSA with RAL above L/P of 2.0 up to 6.0 revealed that a binding capacity is still far from saturation point. To accurately approach the saturation level, the protein stock solution has been diluted 5-fold and 10-fold to provide concentrations of 8.6 μM and 4.3 μM, and a titration with RAL was performed with the steps by 5 molar equivalent excess of the ligand using 3.3 mM and 6.8 mM RAL stock solutions. Our results therefore, suggest that titration of HSA with retinal is concentration dependent. Comparing the titration of HSA by RAL with that of RA and RAC at the same protein concentration (43.2 μM) lead us to conclude that RAL binds to HSA non-specifically at multiple (as observed, a minimum of six) binding sites.

To further test the possibility that RAL complexation with HSA occurs via Schiff's base formation, equimolar complex HSA–RAL was acidified with 1 M HCl (~20 equiv.). This results in a bathochromic (25 nm) shift in the absorption spectrum and a better spectral stability, typical for protonated Schiff's bases.

3.2. CD measurements

3.2.1. Far-UV CD (200–260 nm)

The samples of the titration sets for each of the ligands (RA, RAL and RAC) have been subjected to far-UV CD measurements. Fig. 4 shows CD spectra in 200–260 nm range for the control HSA sample and the same protein preparation complexed with 0.1, 0.8, and 2.0 molar equivalents of RA.

3.2.2. Visible CD (300–600 nm)

While a conventional protein CD in 200–260 nm range (Fig. 4) does not show any significant conformational changes upon complexation of HSA with RA, the visible CD range (300–600 nm)

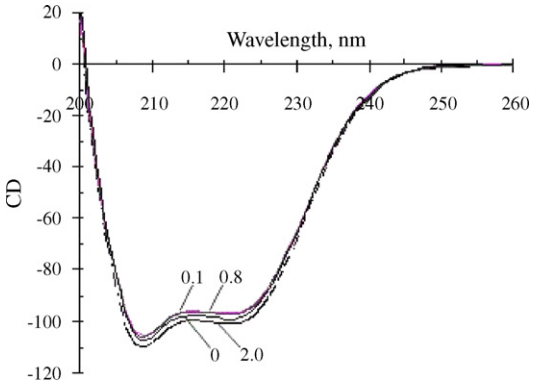

Fig. 4 – Far-UV CD spectra of HSA in PBS (control, curve 0), and of HSA–RA complexes of L/P ratio 0.1, 0.8 (overlapped) and 2.0, respectively. (Concentration of HSA in these samples was 4.3 μM; pathlength 2 mm.)

reveals the dramatic conformational changes of the ligand due to a protein-induced chirality (Figs. 5 and 6).

3.2.2.1. Dynamics of the HSA–RA complex formation. Fig. 5 illustrates the dynamics of the early stages of the complex formation between RA and HSA (L/P of 1.0 is shown). Both the absorption and CD spectra reflect an instant association of the ligand with protein, however, CD provides more details on dynamics of the interaction. Upon adding of RA, the absorption spectra instantly reflects a bathochromic shift to 365 nm with a broad shoulder at ~420–430 nm that corresponds to RA aggregation. That is followed rapidly (~14 min) by a major band shift back to ~353 nm while retaining some absorption at 420 nm. By 40 min, the absorption shoulder at 420 nm completely disappeared, while the absorption maximum at 353 nm has reached its maximal intensity.

As an optically inactive molecule, RA itself does not exhibit any CD, either in ethanol and in buffer. HSA also does not show any CD in the visible range. An optical activity in the visible range is observed only when RA is added to HSA solution.

CD spectra measured for earlier steps of binding, clearly illustrate that although RA has a high affinity to HSA and

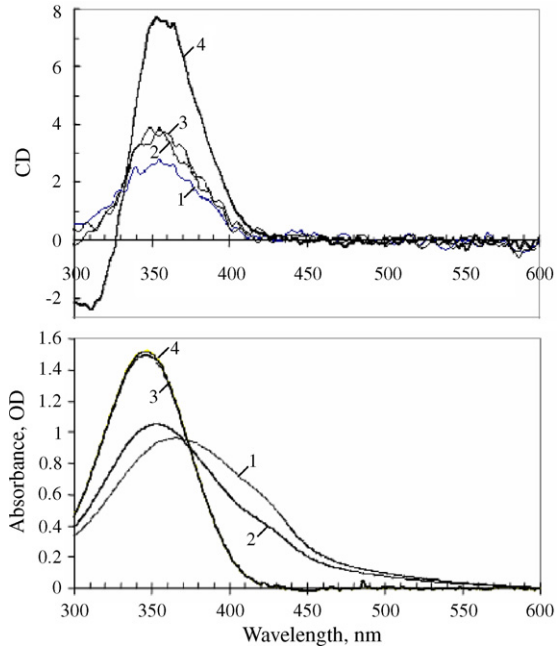

Fig. 5 – Dynamics of the RA binding to HSA as monitored by UV–vis absorption and visible CD: 1 min (trace 1), 14 min (trace 2), 40 min (trace 3), and 4 h (trace 4).

rapidly associates with it, a full accommodation of the ligand inside the protein binding site(s) takes several hours. A fine structure of the CD spectra during monitoring of the binding reflects the chromophore conformational alterations due to ongoing dynamic changes. All CD spectra recorded for the first 2 h of binding exhibit only a major positive band of fine structure around 350 nm. Four hours later, the reaction results in a relatively smooth biphasic CD spectrum that is comprised of two bands: a major positive CD at ~350–355 nm (positive 1st CE), followed by a small negative CD around 314 nm (negative 2nd CE). These spectra are reproducible and do not change over weeks.

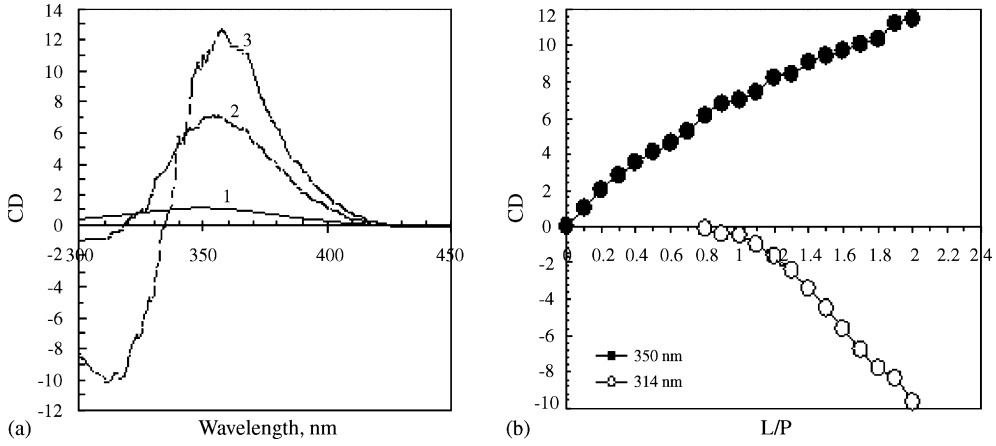

Fig. 6 – (a) CD of HSA complexes with RA of L/P 0.1 (curve 1), 0.8 (curve 2) and 1.95 (curve 3); (b) plot of the CD intensities at 350 nm and 314 nm for titration of HSA with RA as a function of L/P. (CD spectrum of 43.2 μM HSA was subtracted.)

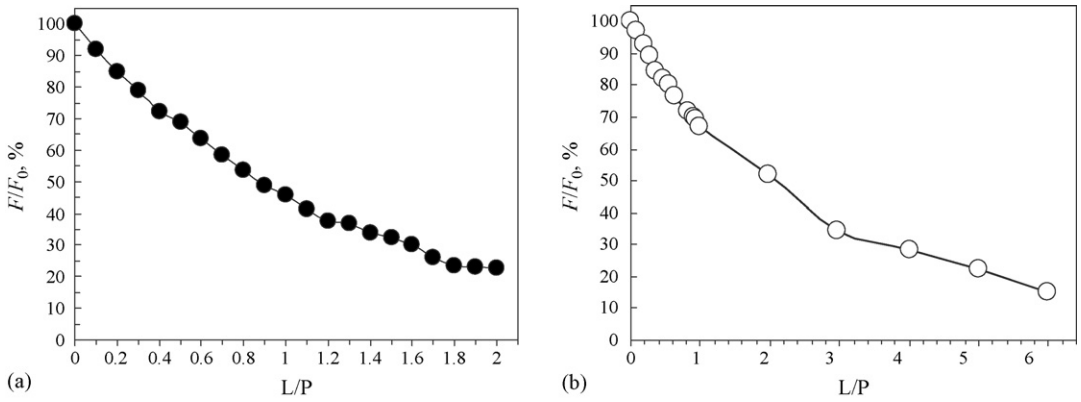

Fig. 7 – Quenching of the intrinsic HSA fluorescence due to titration with RA (a) and RAL (b). Percent of the observed fluorescence intensity at 340 nm (F/F_0) is plotted as a function of L/P.

3.2.2.2. CD spectra of the HSA–RA samples of various L/P ratio (titration). While the UV–vis spectra of HSA with increasing amounts of RA demonstrate a gradual increase in the absorption intensities (Fig. 3a and c), a concentration dependent CD response in the visible range is more informative.

Fig. 6a shows the selected CD spectra to demonstrate the major RA conformational changes depending on amount of RA added per mole of HSA.

For clarity we plotted the intensities of positive and negative Cotton Effects taken at 350 nm and 314 nm for all samples as a function of L/P (Fig. 6b). These CD data are complementary to UV–vis spectra shown in Fig. 3a. From the low L/P (0.1) and up to 0.8 the CD spectra show the only one arising positive CD band (positive CE) which intensities correlate with RA concentrations and the corresponding absorption spectra. It suggests that up to a L/P of 0.8 RA binding proceeds as if there is only a single binding site. However, starting L/P of 0.9, a negative band at ~314 nm is arising, and the spectrum of the equimolar RA–HSA complex already shows a small negative CE as well. The intensity of the negative CE is increasing with increase of RA content in the system (from L/P of 0.9 to 2.0). The intensities of the corresponding positive lobes of the titration CD spectra are increasing and gradually shift from λ_{max} 350 nm to 358 nm. Thus, titration results in an almost conservative biphasic CD spectrum of the fully saturated complex.

3.2.2.3. CD of the complexes of RAL and RAC with HSA. CD measurements for the titration sets of HSA with RAL and RAC did not show any CD in the visible (chromophore) range, thus, indicating that an association of HSA with these chromophores does not induce any CE, and the ligands remain optically inactive.

3.3. *Fluorescence study*

The only tryptophan in HSA (W^{214}), located in the physiologically important subdomain 2A, is predominantly responsible for HSA intrinsic fluorescence.

We have performed fluorescence study for the titration sets with each ligand. Fig. 7a shows a plot of the fluorescence intensities for the HSA–RA titration samples. The adding of increasing amounts of RA results in a gradual reduction of the emission intensity.

Upon saturation of HSA with RA (at L/P close to 2.0), the remaining unquenched fluorescence is ~22–23% of initial intrinsic protein fluorescence. The fluorescence intensity profile for the HSA–RA titration set shows that 76% of quenching of the intrinsic fluorescence corresponds to adding of the first RA equivalent (L/P of 0.8–1.0), while further saturation of protein with RA (L/P ratio from 1.2 to 2.0) has much lower influence on fluorescence. Thus, this suggests proximity of the RA primary binding site to the W^{214} residue. The affinity constant for the primary binding site for RA was determined using traditional Skatchard plots[2] [31,32], with the resulting value close to that recently published by Maiti et al. from their fluorescence study [27].

Despite lower stability of the complexes with RAL and RAC, we have performed an evaluation of the fluorescence quenching by these ligands. Fig. 7b shows the fluorescence quenching profile for HSA–RAL samples of the L/P ratio up to 6.0. It suggests that RAL, while apparently associated on the protein exterior, may influence the protein intrinsic fluorescence. At a L/P of 6.0, HSA intrinsic fluorescence is almost completely suppressed by non-specifically bound RAL. However, in comparison with the influence of RA on the intrinsic fluorescence of albumin (Fig. 7a), the influence of RAL for the samples of the same L/P is significantly lower.

3.4. *UV–vis time course measurements*

Fig. 8a shows percent of the initial absorbance of the equimolar mixtures of HSA with RA, RAL and RAC as measured over a period of 10 days at their λ_{max}. A superior reproducibility of HSA–RA absorption intensity additionally confirms a strong highly specific binding of RA. Moreover, Fig. 8b overlays the spectra measured for HSA–RA equimolar sample on 20 h after adding RA and 3 months later, thus reflecting a stability of the complex. It is worthwhile to study

[2] Scatchard plot analyses based on fluorescence titration data, UV–vis absorption titration, and CD titration data, are not shown here to be considered in a separate manuscript.

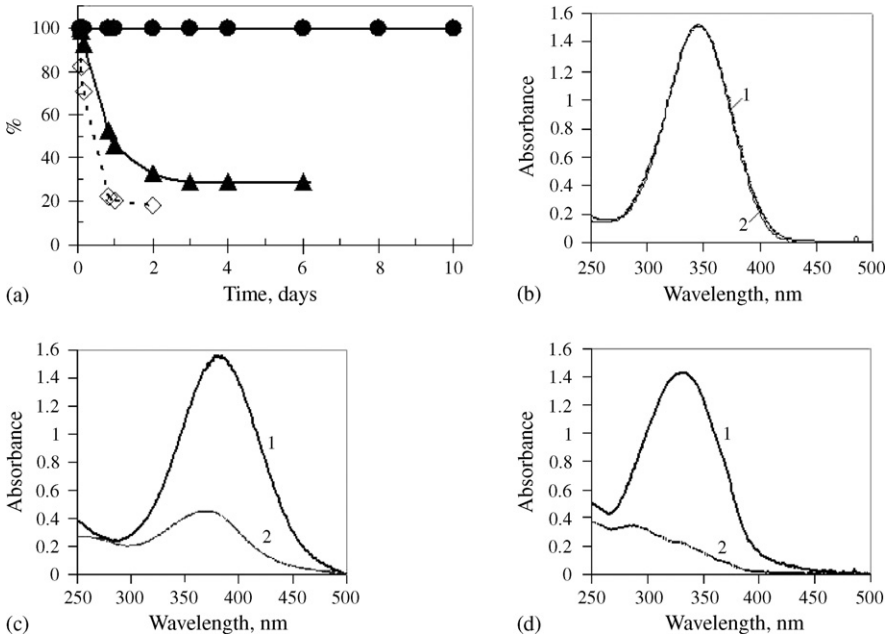

Fig. 8 – UV–vis data for equimolar mixtures of HSA with RA, RAL and RAC: (a) monitoring of the absorbance intensities shown as a percent of the remaining initial absorbance at λ_{max} (RA: bold circles, RAL: bold triangles, and RAC: rhombic dashed trace); UV–vis spectra of equimolar mixtures of HSA with (b) RA: 1 h after mixing (1) overlaid with its spectrum taken 3 months later (2); (c) RAL: 1 h after mixing (1) overlaid with its spectrum taken 6 days later (2); (d) RAC: 1 h after mixing (1) overlaid with its spectrum taken 20 h later (2). The samples were stored in PBS at 4 °C. (Initial spectrum of HSA is subtracted from all spectra.)

whether RA, in its turn, does stabilize the protein, similar to fatty acids [33,34].

RAL and RAC both show rapid clearance from HSA-containing solutions, but at different rates (Fig. 8a). Within 6 days of storage in the original solution, RAL still displays ~30% of initial absorbance intensity and UV–vis spectrum of regular shape, but blue-shifted (Fig. 8c), while RAC precipitates from the solution much faster (Fig. 8c).

4. Discussion

Three retinoids, RA, RAC, and RAL, were studied in terms of their affinity to HSA. Our data show that all three retinoids exhibit an affinity to HSA and non-covalently associate with the protein, but the nature of this association significantly differs. Despite their exclusive structural similarity, RA is the only ligand that forms true complexes with HSA by specifically occupying the internal binding sites. The differences between RA, RAL and RAC in terms of specific binding to HSA must be attributed to their functional groups. As a polyunsaturated fatty acid, RA is expected to interact with HSA at the fatty acid (FA) binding sites. Interactions of RA with bovine serum albumin have been well characterized. Earlier work on bovine serum albumin reported three binding sites for RA [35,36], and two of these sites may be FA binding sites [12]. Later, Nerli and Pico reported on two types of binding sites for bovine serum albumin with affinity constants of $10^5\ M^{-1}$ and $10^4\ M^{-1}$, respectively [31]. They also showed that RA binds to the FA binding sites, producing a perturbation in both principal drug binding sites of the protein.

However, the interactions of RA with HSA, the major human plasma protein and a widely used therapeutic, have not been thoroughly investigated. In 2006, Maiti et al. [27] reported that RA binds to HSA to one class of sites on the protein with an average n value of 0.97 (the binding stoichiometry per class of binding site), as well as provided data to suggest the docking of one RA molecule per HSA. However, according to our results, RA binds to HSA with maximal stoichiometry of 2 mol of RA per 1 mol of HSA, and our data confirm the existence of at least two binding sites. It is of note that the observed stoichiometry does not exclude an existence of more than two RA-binding sites that, e.g., are not achievable because of steric hindrance, cooperative conformational changes, or require a higher concentration level of free RA. Although the affinities of the binding sites may vary significantly, the filling of the primary binding site does not proceed without a certain random scrambling of the ligand to other sites. Crystal structure may ultimately confirm which FA binding sites are more preferable for RA and whether it can bind to HSA at more than two sites (e.g., similar to myristic or arachidonic acid [5,37]).

The main focus of this study was to examine interactions of the chromophoric ligands with protein binding sites by visible CD. While CD in the far-UV range does not show any significant protein conformational alterations upon adding retinoids, visible CD reveals dramatic spectral changes in case of RA.

Retinoids are optically inactive molecules and thus, they exhibit zero CD in the visible range both in ethanolic and aqueous solutions. The protein also shows zero CD in the visible range, while exhibiting its optical activity in far- and near-UV. Therefore, an optical activity observed upon titration of HSA with RA in the visible range reflects a well-known phenomenon of protein-induced chirality [38–41], suggesting acquisition of optical activity by RA due to interactions with the asymmetric protein binding site(s).

The induced CD spectra observed upon titration of HSA with RA, indicate that RA accommodates in an asymmetric protein binding site (or sites), thus adopting a chirality of the helical host via steric interactions with amino acid residues of the binding site. As a result, being bound to the protein, RA behaves as a chiral molecule and exhibits an optical activity in the region of its absorption maximum.

The induced optical activity observed for RA upon binding HSA provides an insight into the dynamics of its interaction with HSA and gives valuable information on RA interactions with protein binding sites, as well as suggests a chromophore–chromophore *exciton coupling* between the RA molecules within the protein.

CD study of the early stages of interaction showed that binding of RA to a specific binding site requires several (~4) hours. The interaction of RA with protein during initial steps of the complexation is reflected by the immediately arising band of the positive CE around 350 nm. For equimolar HSA–RA sample, the visible CD visualizes that it first proceeds at a single binding site showing a single arising positive CE, then followed by delayed appearing of the second (negative) CE when more RA timely gets into the system.

CD study of HSA titration with RA is an additional manifestation of highly specific binding with HSA (Fig. 6). From ligand-to-protein ratio 0.1 to 0.8, an increasing single broad positive CE is the only one trend observed upon increasing amount of RA, which very likely points out the predominant occupying of the first binding site.

Moreover, a significant finding of this work is that a higher saturation of HSA with RA gradually leads to a strong bisignate CD, a hallmark of an exciton coupling between the dipole transition moments of the chromophores [38,39,42]. Starting L/P of 0.9 and up to 2.0, CD spectra show arising negative Cotton Effect, thus reporting on a strong influence of the appearing of the second molecule of RA in the system. It suggests that two RA molecules within the protein are chirally disposed in regard to each other and may efficiently interact through the space.

The intramolecular distances between the principal binding sites inside HSA (~20–35 Å) do allow chromophore–chromophore interactions within the protein [39,42,43]). The presence of a third distinct chromophore, tryptophan at the position 214, also should be taken into account [30,44], generally regarding the first CE. However, its energetic level differs from that of RA, which enables us to postulate that the appearance of the bisignate CD is caused mainly by the exciton coupling between two RA molecules in the protein interior bound at different binding sites.

Although RAL and RAC also showed an association with HSA, they remain optically inactive, indicating the absence of conformational distortion by the protein, thus implicating surface type of association with HSA. In view of completely neutral nature of retinyl acetate, in which the functional group is esterified, its association with HSA can be explained exclusively via hydrophobic interactions, probably at the protein surface clefts.

RAL complexed with HSA does not exhibit an optical activity either, thus also indicating a surface type of complexation. However, interactions of RAL with protein are more intriguing. In view of reactivity of retinal aldehyde group and multiple non-specific binding observed, a mechanism of interaction of RAL with protein can be either (a) via hydrogen bond network, or (b) formation of the reversible Schiff's base between the aldehyde and the ε-amino groups of the accessible lysine residues (e.g., [45,46]). We favor the latter hypothesis, since acidifying of HSA–RAL complexes results in more stable adducts with red-shifted (~25 nm) absorption spectra, typical for protonated Schiff's bases. However, in case of RAL, besides multiple non-specific binding with ε-amino groups of the accessible lysine residues, we did not exclude a possibility to observe the signs of binding at the same internal sites that worked for RA molecules, due to Schiff's base formation with ε-amino group of lysine inside of binding site [2]. The absence of any induced CE in the protein titration with RAL clearly indicates that, despite its exclusive structural similarity to RA and higher reactivity of its functional group, RAL does not get into the same binding sites that RA does.

In summary, our study clearly demonstrates that RA specifically binds to HSA with stoichiometry up to 2 mol of RA per 1 mol of protein, and that there are at least two RA binding sites of close but distinct affinities. The observed protein-induced chirality, revealed by visible CD, together with fluorescence quenching data indicate that RA occupies two (or more) internal binding sites, and the primary binding site is close to W^{214}. Moreover, biphasic CD spectra observed for the complexes of L/P ratios of 0.9–2.0, suggest intramolecular exciton coupling between two RA molecules while occupying their binding sites in the protein interior. A highly specific binding of RA with albumin is additionally confirmed by exclusive stability of these complexes.

RAC shows an association with HSA with a stoichiometry close to that of RA, but zero CD indicates the absence of conformational distortions of chromophore, which together with its clearance profile, implicate a weak hydrophobic interaction with the protein presumably at the surface.

RAL displays a non-specific interaction with HSA at multiple binding sites, most likely via formation of reversible Schiff's bases with ε-amino groups of the accessible lysine residues. The absence of any sign of the induced CD indicates an exterior type of binding exclusively, confirming that, although RAL is capable of interacting with lysine residues, but not with those which are strategically located inside the internal binding sites. The latter suggests that contrary to RA, the RAL does not get into the RA binding sites.

Thus, our study confirms that the presence of the carboxyl group in RA is a stringent requirement for a highly specific binding of retinoid with HSA. Although the RA carboxyl group is not as reactive as the carbonyl group of RAL, in its ionized form it can enhance initial hydrophobic interactions with protein microenvironment inside the binding site via electrostatic interactions. In comparison with more reactive RAL, the

carboxyl group of RA seems to be indispensable in the navigation of the retinoid agent into the binding channel, which is observed for RA, but nor for RAL.

The *in vitro* binding capacity of HSA for RA allows to consider this therapeutic protein as an efficient carrier for RA for those cases in which a requirement for high doses of RA is hard to be fulfilled because of its low solubility in physiological fluids.

Methodologically, this study can serve as an additional illustration of the use of the visible CD for examining various interactions between native plasma proteins, protein therapeutics, and small chemical drugs and/or native plasma metabolites.

Acknowledgements

The author is grateful to Dr. Abdu Alayash for valuable discussions and critical reading of the manuscript and to Dr. Robert Fisher for his helpful comments. EK thanks Dr. Emily Shacter and Dr. Daron Freedberg for permission to use their equipment.

REFERENCES

[1] Carter D, Ho JX. Advances in protein chemistry, vol. 45. New York: Academic Press; 1994. pp. 153–203.
[2] Peters Jr T, editor. All about albumin: biochemistry, genetics and medical applications. San Diego: Academic Press; 1996.
[3] Fasano M, Curry S, Terreno E, Galliano M, Fanali G, Narciso P, et al. The extraordinary ligand binding properties of human serum albumin. Critical review. IUBMB Life 2005;57(12):787–96.
[4] Bertucci C, Domenici E. Reversible and covalent binding of drugs to human serum albumin: methodological approaches and physiological relevance. Curr Med Chem 2002;9:1463–81.
[5] Curry S, Mandelkow H, Brick P, Franks N. Crystal structure of human serum albumin complexed with fatty acid reveals an asymmetric distribution of binding sites. Nat Struct Biol 1998;5:827–35.
[6] Bhattacharya AA, Grune T, Curry S. Crystallographic analysis reveals modes of binding of medium and long-chain fatty acids to human serum albumin. J Mol Biol 2000;303:721–32.
[7] Huang BX, Dass C, Kim H-Y. Probing conformational changes of human serum albumin due to unsaturated fatty acid binding by chemical cross-linking and mass spectrometry. Biochem J 2005;387:695–702.
[8] Rang HP, Dale MM, Ritter JM, Moore P. Pharmacology, 5th ed., New York: Churchill Livingstone; 2003, 816 p.
[9] Guidas LJ, Sporn MB, Roberts AB. Cellular biology and biochemistry of retinoids. In: Sporn MB, Roberts AB, Goodman DS, editors. The retinoids: biology, chemistry and medicine. 2nd ed., New York: Raven Press; 1994. p. 443–520.
[10] Lane MA, Bailey SJ. Role of retinoid signalling in the adult brain. Prog Neurobiol 2005;75:275–93.
[11] Dräger UC. Retinoic acid signaling in the functioning brain. Sci STKE 2006;10.
[12] Mangelsdorf D, Umesono K, Evans R. The retinoid receptors. In: Sporn MB, Roberts AB, Goodman DS, editors. The retinoids: biology, chemistry and medicine. 2nd ed., New York: Raven Press; 1994. p. 319–50.
[13] Noy N. Retinoid-binding proteins: mediators of retinoid action. Review. Biochem J 2000;348:481–95.
[14] Noy N. The ionization behavior of retinoic acid in aqueous environments and bound to serum albumin. Biochim Biophys Acta 1992;1106:152–8.
[15] Han CH, Wiedmann TS. Spectral properties and ion dissociation behavior of retinoids. I. Aqueous solutions. Int J Pharm 1988;172:241–53.
[16] Szuts EZ, Haroshi FI. Solubility of retinoids in water. Arch Biochem Biophys 1991;287(2):297–304.
[17] Penniston KL, Tanumihardjo SA. The acute and chronic toxic effects of Vitamin A. Am J Clin Nutr 2006;83:191–201.
[18] Hong WK, Itri LM. Retinoids and human cancer. In: Sporn MB, Roberts AB, Goodman DS, editors. The reinoids: biology, chemistry, and medicine. 2nd ed., New York: Raven Press; 1994. p. 597–630.
[19] Hansen LA, Sigman CC, Andreola F, Ross SA, Kelloff GJ, De Luca LM. Retinoids in chemoprevention and differentiation therapy. Carcinogenesis 2000;21:1271–9.
[20] Okuno M, Kojima S, Akita K, Matsushima-Nishiwaki R, Adachi S, Sano T, et al. Retinoids in liver fibrosis and cancer. Review. Front Biosci 2002;7:d204–18.
[21] Conley B, Egorin M, Sridhara R, Finley R, Hemady R, Wu S, et al. Phase I clinical trial of *all-trans*-retinoic acid with correlation of its pharmacokinetics and pharmacodynamics. Cancer Chemother Pharmacol 1997;39:291–9.
[22] Frankfurt O, Tallman MS. Strategies for the treatment of acute promyelocytic leukemia. J Natl Comp Network 2006;4(1):37–50.
[23] Einspahr JG, Stratton SP, Bowden GT, Alberts DS. Chemoprevention of human skin cancer. Crit Rev Oncol Hematol 2002;41:269–85.
[24] Kaiser PC, Körner M, Kappeler A, Aebi S. Retinoid receptors in ovarian cancer: expression and prognosis. Ann Oncol 2005;16:1477–87.
[25] Furr HC, Barua AB, Olson JA. Analytical methods. In: Sporn MB, Roberts AB, Goodman DS, editors. The retinoids: biology, chemistry and medicine. 2nd ed., New York: Raven Press; 1994. p. 179–211.
[26] Saurat JH, Didierjean L, Masgrau E, Piletta PA, Jaconi S, Chatellard-Gruaz D, et al. Topical retinaldehyde on human skin: biologic effects and tolerance. J Invest Dermatol 1994;103:770–4.
[27] Maiti TK, Ghosh KS, Debnath J, Dasgupta S. Binding of all-*trans* retinoic acid to human serum albumin: fluorescence FT-IR and circular dichroism studies. Int J Biol Macromol 2006;38(3–5):197–202.
[28] Gundersen TE, Blomhoff R. Qualitative and quantitative liquid chromatographic determination of natural retinoids in biological samples. J Chromatogr A 2001;935:13–43.
[29] Hemley R, Kohler BE. Electronic structure of polyenes related to the visual chromophore. A simple model for the observed band shapes. Biophys J 1977;20:377–82.
[30] Zsila F, Bikadi Z, Simonyi M. Retinoic acid binding properties of the lipocalin member β-lactoglobulin studied by circular dichroism, electronic absorption spectroscopy and molecular modeling methods. Biochem Pharmacol 2002;64:1651–60.
[31] Nerli B, Pico G. Use of retinoic acid as a fluorescent probe to study conformational change of the albumin molecule. Biochem Mol Biol Int 1994;32(4):781–8.
[32] Paal K, Muller J, Hegedus L. High affinity binding of paclitaxel to human serum albumin. Eur J Biochem 2001;268:2187–91.
[33] Anraku M, Tsurusaki Y, Watanabe H, Maruyama T, Kragh-Hansen U, Otagiri M. Stabilizing mechanisms in commercial albumin preparations: octanoate and *N*-acetyl-L-tryptophanate protect human serum albumin against

heat and oxidative stress. Biochim Biophys Acta 2004;1702:9–17.
[34] Shrake A, Frazier D, Schwarz FP. Thermal stabilization of human albumin by medium- and short-chain *n*-alkyl fatty acid anions. Biopolymers 2006;81(4):235–48.
[35] Lehman ED, Spivey HO, Thayer RH, Nelson EC. The binding of retinoic acid to serum albumin in plasma. Fed Proc (Fed Am Soc Exp Biol) 1972;31:A672.
[36] Smith JE, Milch PO, Muto Y, Goodman DS. The plasma transport and metabolism of retinoic acid in the rat. Biochem J 1973;132:821–7.
[37] Petitpas I, Grune T, Bhattacharya AA, Curry S. Crystal structures of human serum albumin complexed with monounsaturated and polyunsaturated fatty acids. J Mol Biol 2001;314:955–60.
[38] Harada N, Nakanishi K. Circular dichroic spectroscopy—exciton coupling. In: Organic stereochemistry. Mill Valley, CA: University Science Books; 1983. pp. 85–88.
[39] Berova N, Nakanishi K. Principles and applications of exciton chirality method. In: Berova N, Nakanishi K, Woody R, editors. Circular dichroism, principles and applications. New York: Wiley-VCH; 2000. p. 337–82.
[40] Lightner DA, Gurst JE. Organic conformational analysis and stereochemistry from circular dichroism spectroscopy. New York: Wiley-VCH; 2000. pp. 423–456.
[41] Zsila F, Bikadi Z, Fitos I, Simonyi M. Probing protein binding sites by circular dichroism spectroscopy. Curr Drug Discov Tech 2004;1:133–53.
[42] Berova N, Borhan B, Dong JG, Huang X, Karnaukhova E, Kawamura A, et al. Solving challenging bioorganic problems by exciton coupled CD. Pure Appl Chem 1998;70:377–83.
[43] Karnaukhova E, Vasileiou C, Wang A, Berova N, Nakanishi K, Borhan B. Circular dichroism of heterochromophoric and partially regenerated purple membrane: search for exciton coupling. Chirality 2006;18:72–83.
[44] Fugate RD, Song PS. Spectroscopic characterization of β-lactoglobulin–retinol complex. Biochim Biophys Acta 1980;625:28–42.
[45] Abraham EC. Glycosylated hemoglobins. Clinical and biochemical analysis, vol. 19. New York: Marcel Dekker Inc.; 1985. pp. 1–5.
[46] MacBeath G, Schreiber SL. Printing proteins as microarrays for high-throughput function determination. Science 2000;289:1760–3.